PHYSICAL REVIEW A **78**, 010302(R) (2008)

Demonstration of pure geometric universal single-qubit operation on two-level atoms

Hiromitsu Imai and Atsuo Morinaga
Department of Physics, Faculty of Science and Technology, Tokyo University of Science, 2641 Yamazaki, Noda-shi, Chiba 278-8510, Japan

(Received 27 December 2007; published 2 July 2008)

With carefully prepared resonant laser-controlled pulses, the two quantum states of a cold ensemble of sodium atoms were manipulated by pure geometric rotations of the Bloch vector around axes 2 and 3 on the Bloch sphere. The fidelity for two geometric rotations was improved to be 90%. A universal single-qubit operation on the ground-state wave function was demonstrated by a pure geometric operation and the phase shift due to the rotation around axis 3 was measured using a geometric atom interferometer.

DOI: 10.1103/PhysRevA.78.010302 PACS number(s): 03.67.Lx, 03.65.Vf, 03.75.Dg, 37.10.Gh

Quantum computation is one of the most promising and fascinating subjects that mankind will develop in the 21st century. In order to realize quantum computation, there are two building blocks: one is a universal single-qubit operation and the other is a controlled-NOT gate for two qubits [1]. In particular, the universal single-qubit operation is important, since it is applicable to a basis of a controlled-NOT gate. A universal single-qubit operation is an arbitrary unitary operation on a single qubit of two-level systems such as atoms or spins [2,3]. In a two-level system, it can be accomplished by three successive rotations of the Bloch vector around principal axes 3 and 2 on the Bloch sphere, as shown in Fig. 1(a) [1]. These rotations have generally been induced through dynamic evolution of interaction Hamiltonians from external sources such as laser pulses and magnetic fields, but they can also be induced through a geometric effect. The geometric manipulations are more robust than dynamic ones since a geometric phase depends solely on the amount of the solid angle enclosed by the evolution path, not on the details of the path, the time spent, the driving Hamiltonian, or the initial and final states of the evolution [4]. Up to now, experimental demonstrations using partial geometric operation have been presented in nuclear magnetic resonance [5] and ion trap [6] systems.

In 2004, Tian *et al.* proposed that the Bloch vector can be rotated around axes 3 and 2 by geometric manipulations using resonant laser-controlled pulses [7]. Special closed paths

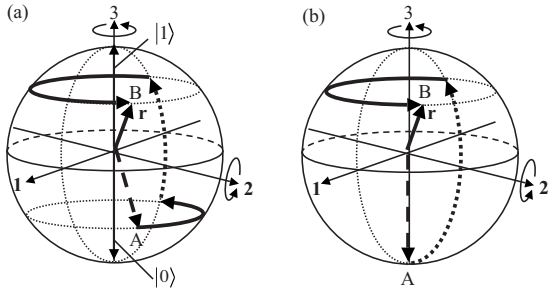

FIG. 1. (a) Trace of Bloch vector **r** driven by universal single-qubit operation. The Bloch vector at initial position A is rotated around axis 3 to the 1-3 plane, varying the phase of the wave function, then rotated around axis 2, changing the population probability of the two states, and rotated around axis 3 to the final position B. (b) Initial position A is the ground-state wave function.

were designed to eliminate the infidelity of the operation associated with the Hamiltonian-dependent dynamic phase. They verified a geometric rotation around axis 3 using heterodyned photon echoes for an ensemble of inhomogeneously detuned two-level Tm^{3+} doped in a yttrium aluminum garnet crystal. The rotation angle was controlled by two resonant laser-controlled π pulses with a relative phase difference of $\delta/2$ and the phase was changed by twice the control phase, as expected.

Recently, we succeeded in demonstrating geometric rotation around axes 3 [8] and 2 [9] using a cold ensemble of sodium atoms. We evaluated that a geometric rotation around axis 3 was twice the control phase change within an uncertainty of 1% by monitoring the phase change using the stimulated Raman atom interferometer composed of the excited and the ground hyperfine states of sodium atoms [8]. Next, a geometric rotation around axis 2 was achieved using three resonant laser-controlled pulses with pulse areas of $\pi/2$, π, and $\pi/2$ and a relative phase difference of $\pi+\delta/2$ in the central pulse. The population probability in the excited state could be changed sinusoidally over five cycles [9], compared with a dynamical evolution such as the Rabi excitation [10].

Thus a single geometric rotation for a single qubit on two-level atoms was found to be very accurate and robust. However, if we apply geometric operations successively more than two times on two-level atoms, the ac Stark shift due to the excitation field and correlations between many pulses will distort the phase and the population probability of the wave function manipulated geometrically. Therefore, careful preparations for resonant laser-controlled pulses are necessary in order to accomplish the universal single-qubit operation with a high fidelity.

In this Rapid Communication, we present first an improvement for preparing the resonant laser-controlled pulse. Next we evaluate the fidelity of the present system from a couple of geometric rotations around the same axis on two-level atoms driven by two resonant laser-controlled pulses. Lastly, as an example of universal single-qubit operation, we demonstrate two geometric rotations around axes 2 and 3 on the ground-state wave function successively, and we measure the phase shift using an atom interferometer constructed of pure geometric operations.

As shown in Fig. 1(a), we consider a two-level atom associated with a wave function A described as $\Psi_A = a|0\rangle$

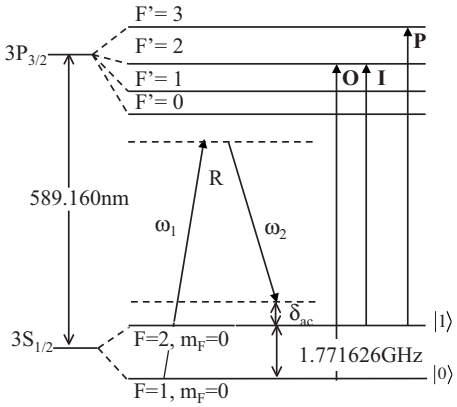

FIG. 2. Partial level scheme and transitions of sodium atoms. R, two-photon Raman transition; I, initializing; P, probe; and O, optical pumping.

$+b|1\rangle$, where $|0\rangle$ represents the ground state ($\mathbf{r}_{-3}$) and $|1\rangle$ is the excited state ($\mathbf{r}_3$). When a universal single-qubit operation is applied to the wave function A, it is transformed to wave function B described as $\Psi_B = a'|0\rangle + b'|1\rangle$. The universal single-qubit operation is equivalent to three successive rotations of the Bloch vector around axes 3, 2, and 3 [1], which can be accomplished as

$$U = U_3(\gamma)U_2(\beta)U_3(\alpha) = \begin{pmatrix} e^{i\gamma/2} & 0 \\ 0 & e^{-i\gamma/2} \end{pmatrix} \begin{pmatrix} \cos(\beta/2) & \sin(\beta/2) \\ -\sin(\beta/2) & \cos(\beta/2) \end{pmatrix} \times \begin{pmatrix} e^{i\alpha/2} & 0 \\ 0 & e^{-i\alpha/2} \end{pmatrix}, \quad (1)$$

where U_3 and U_2 are rotations around axes 3 and 2 of the Bloch sphere, respectively. α β, and γ denote the corresponding rotation angle. With the first rotation around axis 3, the Bloch vector rotates to the 1-3 plane by α, while the probabilities of the excited and the ground states are preserved. With the second rotation around axis 2, the Bloch vector rotates in the 1-3 plane by β and the probabilities of the states are changed. With the third rotation around axis 3, the phase of the Bloch vector rotates by γ to the phase of wave function B from the 1-3 plane. In the special case in which the initial state A is the ground-state wave function, the universal single-qubit operation shortens to two successive rotations around axes 2 and 3, as shown in Fig. 1(b).

We used a laser-cooled ensemble of sodium atoms as a two-level system. The $F=1$, $m_F=0$ and $F=2$, $m_F=0$ states in the ground hyperfine level $S_{1/2}$ were used as the ground state and the excited state, respectively. The two states were coupled with a stimulated Raman transition comprised of nonresonant two-photon transitions, one of which is ω_1 from $3S_{1/2}$, $F=1$, $m_F=0$ to $3P_{3/2}$, $F'=2$, $m_{F'}=1$, and the other is ω_2 from $3P_{3/2}$, $F'=2$, $m_{F'}=1$ to $3S_{1/2}$, $F=2$, $m_F=0$, as shown in Fig. 2. The right-hand circular polarization was used for excitation. The frequency difference between ω_1 and ω_2 was produced using an electro-optic modulator (EOM) driven at around 1.771 626 GHz, which corresponds to the frequency difference between the $F=1$, $m_F=0$ and $F=2$, $m_F=0$ states.

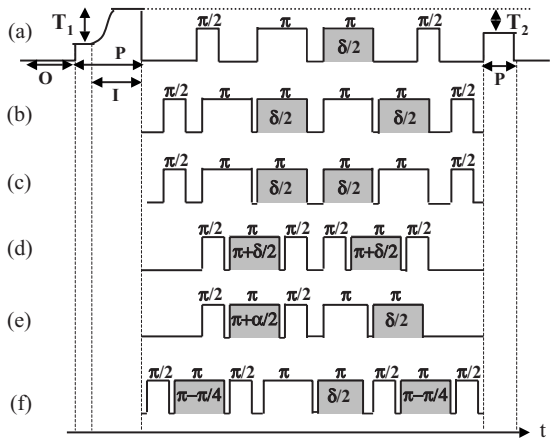

FIG. 3. Resonant laser-controlled pulses of Raman beam. I, initializing; P, probe; O, optical pumping; T_1 and T_2, transmittance. The figure above each pulse shows the pulse area and the figure on the shadow shows the phase shift. (a) Single rotations around axis 3 with atom interferometer (AI), (b) addition of two rotations around axis 3 with AI, (c) subtraction of a rotation around axis 3 and a reverse rotation with AI, (d) addition of two rotations around axis 2, (e) two rotations around axes 2 and 3, and (f) three rotations around axes 2, 3, and 2.

This scheme has a superior feature in that the optical frequency jitter can be canceled out in the atom-laser interaction [10]. Furthermore, atoms were irradiated by two copropagating laser beams to cancel out the recoil momentum due to each optical photon [11].

Using the Raman beam, the resonant laser-controlled pulses for geometric rotations were prepared as follows. The ac Stark shift depending on the intensity of the Raman beam was canceled out by adjusting the ratio of intensities of ω_1 and ω_2 [12]. The output power of the Raman beam was stabilized to be constant. After that, the Rabi oscillation was measured as a function of pulse width at the resonance frequency without ac field, so that the width of the π pulse was determined. The interval between the control pulses was spaced comparing with a risetime of phase change in the EOM. With such careful preparations of the resonant laser-controlled pulses, the phase shift due to the ac Stark shift was canceled out and distortions or decoherence observed in the interference fringes were reduced.

The experimental setup was almost the same as the previous one used for geometric rotation around axes 3 [8] and 2 [9], except for generation of the Raman beam. The ω_2 of the Raman beam was generated independently from the second laser and stabilized to about 600 MHz below the resonance frequency from the $F=2$, $m_F=0$ to $F'=2$, $m_{F'}=1$ states by a frequency offset-lock, and its power was stabilized using an acousto-optic modulator. The difference frequency between ω_1 and ω_2, the intensity ratio of ω_1 and ω_2, and the phase of ω_1 were controlled by an EOM driven by a synthesizer and switched on and off by another acousto-optic modulator. They were controlled by a graphical program language (National Instruments, LabView). A typical condition of a Raman beam used in the present experiment was as follows: the intensity ratio was 1:2.7, the total intensity was 0.1 $\mathrm{mW/mm^2}$, and the width of the π pulse was 40 μs.

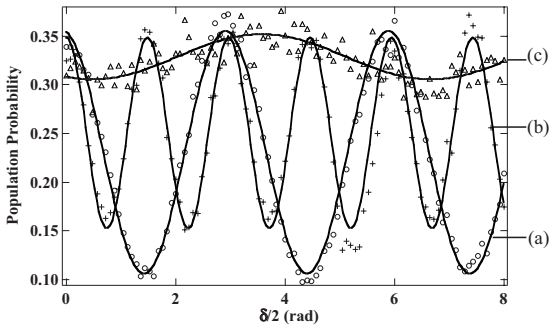

FIG. 4. Interference fringes versus rotations around axis 3 by $\delta/2$. (a) A rotation around axis 3, (b) two rotations around axis 3, and (c) a rotation around axis 3 with a reverse rotation around axis 3.

A typical time sequence of the measurement is shown in Fig. 3(a). After sodium atoms were released from the trap, first all atoms were optically pumped to the $F=2$ state by the optical pumping beam O, and the number of atoms was deduced from the transmittance of the probe beam P, which interacts with atoms in the $F=2$ state. After that, they were prepared perfectly in the $F=1$ state by the initializing beam I. As atoms in the $F=1$ state were distributed equally in three m sublevels under a quantized magnetic field, only one-third of the atoms interacted with two-photon Raman pulses. After interaction, the number of atoms in the $F=2$ state with $m=0$ was deduced again from the transmittance of the probe beam. Then the population probability of the $F=2$ state was obtained from the ratio of the numbers of atoms before and after interaction. Therefore, the maximum population transfer from the $F=1$ state to the $F=2$ state was 33%.

First, we examined the performance for two geometric rotations around the same axis. As an example, we show the interference signals for addition and subtraction of two rotations around axis 3 in Fig. 4, together with that for single rotation. The phase shift between the ground-state and the excited-state wave functions was measured as the variation of the population probability in the excited state using the atom interferometer. Their time sequences of resonant laser-controlled pulses are shown in Figs. 3(a)–3(c). For a single rotation, the population probability varies from 35% to 10% according to the sinusoidal function of $(2.01 \pm 0.02) \times \delta/2$, as shown in Fig. 4(a). The population probability of 35% is almost unity of the expected transfer for the operation. On the other hand, about 10% of the atoms lost coherence through spontaneous emission during a pulse duration of 2π pulse, so that the minimum population probability was limited to 10%. In the interference signal of the addition of two rotations of $\delta/2$ around axis 3, as in Fig. 4(b), the fringe size was decreased to 80% of that for a single rotation due to the width of the 4π pulse, but the phase of fringes shifted sinusoidally with a phase of $(4.03 \pm 0.02) \times \delta/2$. In the case of subtraction in Fig. 4(c), the sinusoidal component of δ could be reduced within scattering of the data, however a small sinusoidal component of $\delta/2$ appeared in the signal of subtraction. It will be generated from the incompleteness of the widths of each pulse. The amplitude of the component of $\delta/2$ was larger than the scattering of the data. Therefore, we defined the present fidelity for two geometric rotations as $1-R$, where R is the ratio of the amplitude of the component of $\delta/2$ on the peak-to-peak amplitude of fringes for two rotations. The fidelity was 90%. If we could remove such a component by appropriate adjustments, the fidelity would be improved still more.

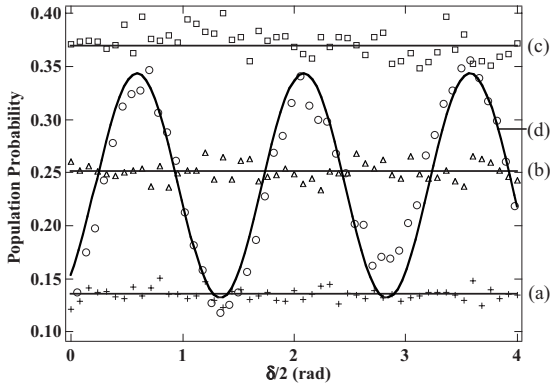

FIG. 5. Population probability of the excited state observed for a sequence of a geometric rotation around axis 2 by $\alpha/2$ and a rotation around axis 3 by $\delta/2$. (a) $\alpha=0$, (b) $\alpha=-\pi/2$, and (c) $\alpha=-\pi$. (d) Two geometric rotations around axis 2, as a reference.

Next, we applied two successive geometric rotations around axis 2 by $\alpha/2$ and around axis 3 by $\delta/2$ to two-level atoms, as shown in Fig. 3(e), in order to demonstrate a universal single-qubit operation from the ground-state wave function. At first, the population probabilities in the excited state were measured for $\alpha=0, -\pi/2$, and $-\pi$ as a function of $\delta/2$. Figures 5(a)–5(c) show the results, where a small component of $\delta/2$, as observed in Fig. 4(c), was eliminated in advance. Figure 5(d) shows the population probability for two identical rotations of $\delta/2$ around axis 2 with a time sequence in Fig. 3(d), as a reference. For $\alpha=0$, the population probability is in the vicinity of the maximum of signal (d) for $\alpha=-\pi/2$ at the middle and for $\alpha=-\pi$ at the minimum. These results verify that the population probability does not depend on the operation of a rotation around axis 3.

In order to confirm the phase shift of the Bloch vector by a geometric rotation around axis 3 in the above operation, we

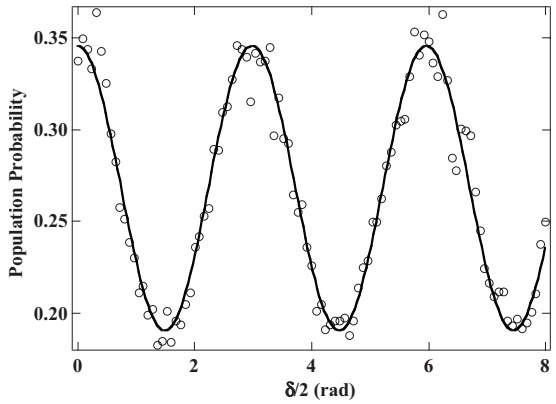

FIG. 6. Phase shift for a universal single-qubit operation. Phase shift due to the rotation around axis 3 by $\delta/2$ was measured by atom interferometer composed of two rotations around axis 2 by $\pi/4$.

constituted an atom interferometer by adding the third geometric rotation of $\pi/4$ around axis 2 together with the first geometric operation of $\pi/4$ around axis 2, as shown in Fig. 3(f). These geometric rotations correspond to the $\pi/2$ pulse of the Rabi excitation. As shown in Fig. 6, the interference fringes of $(2.01 \pm 0.02) \times \delta/2$ appeared clearly, although the fringe size was decreased to 60% of that for a single rotation due to the width of the total 6π pulse. Thus, we could measure the population probability due to the rotation around axis 2 and the phase shift due to the rotation around axis 3 independently. The results confirm orthogonality between geometric rotations around axes 2 and 3. Therefore, we could demonstrate that a universal single-qubit operation on two-level atoms can be accomplished using pure geometric rotations around axes 2 and 3. At the same time, we could construct an atom interferometer using two geometric rotations around axis 2 by $\pi/4$.

In summary, we have prepared precise resonant laser-controlled pulses for geometric rotation around axes 2 and 3, and we determined that the fidelity of the present geometric operation was 90% from addition and subtraction of two geometric rotations around axis 3. Also, we verified the orthogonality of geometric rotations around axes 2 and 3 by measuring the variation of the population probability and the phase shift independently. Finally, as an example of a universal single-qubit operation, successive geometric rotations around axes 2 and 3 of the Bloch vector from the ground state were demonstrated. Thus, we have developed a method of geometric universal single-qubit operations on a cold ensemble of two-level atoms. If we apply geometric operation for a controlled-NOT gate on two qubits, we need two-level systems that are entangled with another superposition state. At present, we are planning to use two-level atoms trapped in an optical lattice entangled with a vibrational state, like ion trap [13].

We thank A. Takahashi and K. Numazaki for assistance in the experiment.

[1] A. Barenco, C. H. Bennett, R. Cleve, D. P. DiVincenzo, N. Margolus, P. Shor, T. Sleator, J. A. Smolin, and H. Weinfurter, Phys. Rev. A **52**, 3457 (1995).

[2] M. A. Nielsen and I. L. Chuang, *Quantum Computation and Quantum Information* (Cambridge University Press, Cambridge, 2000).

[3] T. Calarco, U. Dorner, P. S. Julienne, C. J. Williams, and P. Zoller, Phys. Rev. A **70**, 012306 (2004).

[4] M. V. Berry, Proc. R. Soc. London, Ser. A **392**, 451 (1984).

[5] J. A. Jones, V. Vedral, A. Ekert, and G. Castagnoli, Nature (London) **403**, 869 (2000).

[6] D. Leibfried, B. DeMarco, V. Meyer, D. Lucas, M. Barrett, J. Britton, W. M. Itano, B. Jelenkovic, C. Langer, T. Rosenband, and D. J. Wineland, Nature (London) **422**, 412 (2003).

[7] M. Tian, Z. W. Barber, J. A. Fischer, and Wm. Randall Babbitt, Phys. Rev. A **69**, 050301(R) (2004).

[8] H. Imai, Y. Otsubo, and A. Morinaga, Phys. Rev. A **76**, 012116 (2007).

[9] H. Imai and A. Morinaga, Phys. Rev. A **76**, 062111 (2007).

[10] M. Kasevich and S. Chu, Appl. Phys. B: Photophys. Laser Chem. **54**, 321 (1992).

[11] T. Aoki, K. Shinohara, and A. Morinaga, Phys. Rev. A **63**, 063611 (2001).

[12] D. S. Weiss, B. C. Young, and S. Chu, Appl. Phys. B: Lasers Opt. **59**, 217 (1994).

[13] C. Monroe, D. M. Meekhof, B. E. King, W. M. Itano, and D. J. Wineland, Phys. Rev. Lett. **75**, 4714 (1995).